INTERNATIONAL JOURNAL OF PRECISION ENGINEERING AND MANUFACTURING Vol. 16, No. 7, pp. 1561-1570 JUNE 2015 / 1561
DOI: 10.1007/s12541-015-0206-y ISSN 2234-7593 (Print) / ISSN 2005-4602 (Online)

Trajectory Generation and Sliding-Mode Controller Design of an Underwater Vehicle-Manipulator System with Redundancy

Donghee Kim[1,#], Hyeung-Sik Choi[2], Joon-Young Kim[2], Jong-Hyeon Park[3], and Ngoc-Huy Tran[1]

1 Department of Mechanical Engineering, Korea Maritime and Ocean University, 727, Taejong-ro, Yeongdo-gu, Busan, 606-791, South Korea
2 Division of Mechanical Engineering, Korea Maritime and Ocean University, 727, Taejong-ro, Yeongdo-gu, Busan, 606-791, South Korea
3 School of Mechanical Engineering, Hanyang University, 222, Wangsimni-ro, Seongdong-gu, Seoul, 133-791, South Korea
Corresponding Author / E-mail: risingsun4@kmou.ac.kr, TEL: +82-51-410-4965, FAX: +82-51-404-4350

KEYWORDS: Underwater vehicle-manipulator system, Redundancy resolution, Motion control, Sliding mode control

An Underwater Vehicle-Manipulator System (UVMS) can be applied to pick up and carry objects for autonomous manipulation in the water. However, it is difficult to control the motion of the whole system because the movement of a manipulator affects the motion of the vehicle and vice versa. Additionally, a lack of information about the object, such as the shape and inertia, makes motion control even more difficult. In the current paper, a motion control algorithm of the UVMS with redundancy was developed to guarantee the stability robustness when the mass information of the objects is not available. In order to generate the joint trajectories of the manipulator, a redundancy resolution was performed to minimize the restoring moments acting on the vehicle. This means the propulsion energy for controlling the vehicle's motion can be reduced. To control the motion of the system with an unknown parameter, a controller based on the sliding mode theory has been designed. Finally, the effectiveness of the proposed method was verified through a series of simulation for a 3DOF vehicle-3DOF manipulator system.

Manuscript received: July 21, 2014 / Revised: April 1, 2015 / Accepted: May 10, 2015

NOMENCLATURE

[u, v, w] = translational velocity vector of the vehicle
[p, q, r] = rotational velocity vector of the vehicle
M_{RB} = rigid body inertia matrix
M_A = added mass and inertia matrix
C_{RB} = rigid body Coriolis and centripetal matrix
D_A = hydrodynamic damping matrix
G_v = restoring forces and moments vector
τ_v = external forces and moments vector for the vehicle
R = rotation matrix
η = position vector of the vehicle w.r.t. the Earth-fixed frame
q = joint variable vector of the manipulator system
τ_m = joint torque vector of the manipulator system
F = thruster force vector
J = Jacobian matrix
J_P = performance index function
r_{CG} = position vector to the center of mass
r_{CB} = position vector to the center of buoyancy

1. Introduction

A Remotely Operated Vehicle (ROV) is an underwater vehicle physically linked through a tether with a surface ship. The control commands from an operator as well as the power are transmitted to the vehicle via the tether. On the other hand, an Autonomous Underwater Vehicle (AUV) is supposed to be completely autonomous with its own onboard power and control system. In case of tasks that require interaction with the environment such as picking up an object and removing rust on a ship,[9] the vehicle can be equipped with manipulator links. In this case the system is usually called an Underwater Vehicle-Manipulator System (UVMS).

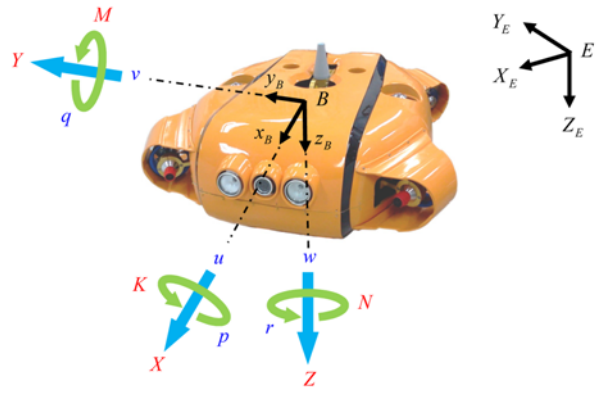

Fig. 1 Coordinate systems of an AUV

When various tasks are performed using an UVMS, it becomes important to control the position of an end-effector accurately. In general, for a base-fixed manipulator system, an inverse kinematics analysis is done to determine the desired joint trajectories of a manipulator based on the given trajectory of an end-effector. However, an UVMS is not fixed at the ground and floats freely under water. Hence, knowledge of the position and orientation trajectory of a vehicle, as well as the trajectory of an end-effector is necessary for calculating the desired joint trajectories of a manipulator through the inverse kinematics analysis. In most of the previous studies, the desired position trajectory of a vehicle was given as a set-point and the control algorithms for station keeping were designed.

If the trajectory of a vehicle is not given in advance, the system has a redundancy and it has an infinite number of solutions in an inverse kinematics. Therefore, when some specified tasks are performed, the redundancy resolution is introduced to determine the desired joint trajectories of a manipulator. The redundant vehicle-manipulator system can have various combinations of joint velocities that do not affect the given velocity profile of an end-effector and this may induce a self-motion of a vehicle. Many past studies had shown that the redundancy may be used to optimize the performance index such as manipulability, energy efficiency, and stability. The redundancy resolution was adopted to avoid the singularity[8] and this concept was also used to determine the task priority during working.[1,2] Furthermore, it was used to generate the desired trajectory so as to minimize the drag force[11] and joint torques.[7] The joint trajectories were generated to minimize the restoring moments.[6] Han's algorithm offers the advantage, which it is easy to apply to the real system, because the parameters such as mass, buoyancy, center of mass, and center of buoyancy are more easily and exactly obtained than are hydrodynamic parameters. However, arbitrary values for the roll and pitch directions can be generated through this algorithm because there are no rules for the generation of the vehicle's attitude. A large amount of roll and pitch angles might cause the instability of the whole system when this system is applied to the special tasks. Moreover, the manipulator arms have to be folded as closely as possible toward the hull of the vehicle to minimize the distance between the mass center and buoyancy center. This situation might cause the joint limitation of the manipulator arms.

In this study, the enhanced performance index is presented to avoid the joint limits and the constraint for a neutral attitude is added to the performance index to improve the stability of the underwater vehicle. Although many studies were performed in the past on optimization of redundant manipulators to find the optimal trajectory, an analysis on the manipulator to perform a task, such as picking up an object was not taken into account. To address this issue, the current paper reports on how a manipulator can deliver an object of unknown mass. In order to control the system, efforts have been devoted to suitably design the sliding mode controller, which would follow the desired trajectory, determined through the redundancy resolution with minimizing the restoring moments. Simulations were conducted to verify the availability of the generated trajectories and performance of the designed controller.

2. Dynamic Modeling

2.1 Dynamics of AUV

To derive the dynamic equations for an AUV, the two coordinate systems are defined as indicated in Fig. 1. *EXYZ* represents the Earth-fixed coordinate system and *Bxyz*, which is attached the center of buoyancy of an AUV, represents the body-fixed coordinate system.

In the body-fixed coordinate system, the positive *x*-direction is the longitudinal axis directed from the stern to the bow, the positive *y*-direction is the transverse axis directed to the starboard, and the positive *z*-direction is the normal axis directed from the top to the bottom. The six Degrees of Freedom (DOF) nonlinear equations of motion for an AUV are described in Eq. (1).[5]

$$\begin{aligned}
&m[\dot{u}-vr+wq-x_G(q^2+r^2)+y_G(pq-\dot{r})+z_G(rp+\dot{q})]=X\\
&m[\dot{v}-wp+ur-y_G(r^2+p^2)+z_G(qr-\dot{p})+x_G(pq+\dot{r})]=Y\\
&m[\dot{w}-uq+vp-z_G(p^2+q^2)+x_G(rp-\dot{q})+y_G(qr+\dot{p})]=Z\\
&I_{xx}\dot{p}-(I_{yy}-I_{zz})qr-I_{yz}(q^2-r^2)+I_{xy}(rp-\dot{q})-I_{zx}(pq+\dot{r})\\
&\quad+m[y_G(\dot{w}-uq+vp)-z_G(\dot{v}-wp+ur)]=K\\
&I_{yy}\dot{q}-(I_{zz}-I_{xx})rp-I_{zx}(r^2-p^2)+I_{yz}(pq-\dot{r})-I_{xy}(qr+\dot{p})\\
&\quad+m[z_G(\dot{u}-vr+wq)-x_G(\dot{w}-uq+vp)]=M\\
&I_{zz}\dot{r}-(I_{xx}-I_{yy})pq-I_{xy}(p^2-q^2)+I_{zx}(qr-\dot{p})-I_{yz}(rp+\dot{q})\\
&\quad+m[x_G(\dot{v}-wp+ur)-y_G(\dot{u}-vr+wq)]=N
\end{aligned} \tag{1}$$

where m denotes the mass of a vehicle and I_{ij} are the moments of inertia for each axis of subscripts; x_G, y_G, and z_G denote the vehicle's mass center; X, Y, Z, K, M, and N denote the external forces and moments acting on the vehicle represented in the body-fixed coordinate system. These equations can be expressed in a more compact form as Eqs. (2) and (3).

$$M_{RB}\dot{\nu}+C_{RB}(\nu)\nu=\tau_\nu \tag{2}$$

$$\begin{aligned}
\nu&=[u\quad v\quad w\quad p\quad q\quad r]^T\\
\tau_\nu&=[X\quad Y\quad Z\quad K\quad M\quad N]^T
\end{aligned} \tag{3}$$

where ν is the body-fixed linear and angular velocity vector and τ_ν is a generalized vector of external forces and moments.

The hydrodynamic forces and moments can be classified as added mass forces, hydrodynamic Coriolis and centripetal forces and hydrodynamic damping forces.[5] When underwater vehicles have

accelerations in the water, both the added mass forces and moments, which are proportional to its acceleration, are generated. If the vehicle has port-starboard symmetry, most of the coefficients become zero and the added mass coefficient matrix is represented as in Eq. (4).

$$M_A = \begin{bmatrix} X_{\dot{u}} & 0 & 0 & 0 & 0 & 0 \\ 0 & Y_{\dot{v}} & 0 & 0 & 0 & Y_{\dot{r}} \\ 0 & 0 & Z_{\dot{w}} & 0 & Z_{\dot{q}} & 0 \\ 0 & 0 & 0 & K_{\dot{p}} & 0 & 0 \\ 0 & 0 & M_{\dot{w}} & 0 & M_{\dot{q}} & 0 \\ 0 & N_{\dot{v}} & 0 & 0 & 0 & N_{\dot{r}} \end{bmatrix} \tag{4}$$

When a rigid-body moves through an ideal fluid, the hydrodynamic Coriolis and centripetal forces can always be parameterized such that the hydrodynamic Coriolis coefficient matrix have a skew-symmetric property as Eq. (5). The hydrodynamic damping forces and moments are highly nonlinear and have the coupled functions of both the linear and the angular velocities. However, the terms higher than the second order becomes negligible if it is assumed that the vehicle has planes of symmetry. From the symmetry, the linear and nonlinear hydrodynamic damping coefficient matrix can be written as in Eq. (6).

$$C_A(\nu) = \begin{bmatrix} 0 & 0 & 0 & 0 & -Z_{\dot{w}}w & Y_{\dot{v}}v \\ 0 & 0 & 0 & Z_{\dot{w}}w & 0 & -X_{\dot{u}}u \\ 0 & 0 & 0 & -Y_{\dot{v}}v & X_{\dot{u}}u & 0 \\ 0 & -Z_{\dot{w}}w & Y_{\dot{v}}v & 0 & -N_{\dot{r}}r & M_{\dot{q}}q \\ Z_{\dot{w}}w & 0 & -X_{\dot{u}}u & N_{\dot{r}}r & 0 & -K_{\dot{p}}p \\ -Y_{\dot{v}}v & X_{\dot{u}}u & 0 & -M_{\dot{q}}q & K_{\dot{p}}p & 0 \end{bmatrix} \tag{5}$$

$$\begin{aligned} D_A(\nu) = D_v(\nu) = &-diag\{X_u, Y_v, Z_w, K_p, M_q, N_r\} \\ &-diag\{X_{u|u|}|u|, Y_{v|v|}|v|, Z_{w|w|}|w|, K_{p|p|}|p|, M_{q|q|}|q|, N_{r|r|}|r|\} \end{aligned} \tag{6}$$

In addition to the added mass and hydrodynamic damping forces, underwater vehicles are also influenced by gravity and buoyancy that include hydrostatic forces and moments. The gravitational force is defined as $W=mg$ and act through the center of gravity, where g is the acceleration due to gravity. The buoyancy force acting through the center of buoyancy is defined as $B = \rho g \nabla$, where ∇ is the volume of fluid displaced by the vehicle and ρ is the density of the fluid. The resulting hydrostatic forces and moments or restoring forces are represented by Eq. (7).

$$G_v(\eta) = \begin{bmatrix} (W-B)\sin\theta \\ -(W-B)\cos\theta\sin\phi \\ -(W-B)\cos\theta\cos\phi \\ -(y_G W - y_B B)\cos\theta\cos\phi + (z_G W - z_B B)\cos\theta\sin\phi \\ (z_G W - z_B B)\sin\theta + (x_G W - x_B B)\cos\theta\cos\phi \\ -(x_G W - x_B B)\cos\theta\sin\phi - (y_G W - y_B B)\sin\theta \end{bmatrix} \tag{7}$$

where $\eta = [x, y, z, \phi, \theta, \psi]^T$ denotes the position and orientation vector with coordinates in the Earth-fixed frame; x_B, y_B, and z_B denote the position of the vehicle's buoyancy center. The dynamic equations of an AUV can be expressed in abbreviated simplified form as in Eqs. (8) and (9). In this paper, the simplified planar model constrained in diving plane is adopted to confirm the effectiveness of the designed controllers and joint trajectories, generated by the redundancy resolution.

$$M_v \dot{\nu} + C_v(\nu)\nu + D_v(\nu)\nu + G_v(\eta) = \tau_v \tag{8}$$

$$\begin{aligned} M_v &= M_{RB} + M_A \\ C_v(\nu) &= C_{RB}(\nu) + C_A(\nu) \end{aligned} \tag{9}$$

2.2 Dynamics of underwater manipulator

The dynamic equations of n-link manipulator are often derived using the iterative Newton-Euler algorithm. For example, Eq. (10) represents the force and the moment between two adjacent links including the hydrodynamic effects.[2,3]

$$\begin{aligned} f_i &= R_{i+1}^i f_{i+1} + F_i - m_i g_i + b_i + P_i \\ t_i &= R_{i+1}^i t_{i+1} + T_i + d_{i/i+1} \times (R_{i+1}^i f_{i+1}) \\ &\quad + d_{i/i_c} \times (F_i - m_i g_i + P_i) + d_{i/i_b} \times b_i + H_k \end{aligned} \tag{10}$$

where R is the rotation matrix from the subscript coordinate system to the superscript coordinate system; f_i and t_i represent the resultant force and moment vector at the i-th joint respectively; d is the position vector from the origin of former coordinate system to that of latter coordinate system; b, P and H denote the buoyancy, hydrodynamic forces and moments acting on the link respectively.

In case of the underwater manipulator, the hydrodynamic forces as well as the buoyancy acting on each link must be included in the dynamic equations of manipulator. In the current work, it has been assumed that the underwater manipulator has the link, which is cylindrical in shape and the hydrodynamic forces acting on such cylindrical elements has already been reported in the past.[12] The hydrodynamic forces and moments such as added mass effects, buoyancy, lift/drag forces, and friction forces should act on the link elements. Thus, the dynamic equations for the underwater manipulator can be written in the concrete form as Eq. (11) through a numerical procedure.

$$M_m(q)\ddot{q} + C_m(q,\dot{q})\dot{q} + D_m(q,\dot{q})\dot{q} + G_m(q) = \tau_m \tag{11}$$

where q is the generalized link coordinates vector; M_m is the inertia matrix of the manipulator; C_m is the Coriolis and centripetal terms of the manipulator; D_m is the hydrodynamic lift and damping matrix; G_m represents the restoring forces and moments of the manipulator. In the current paper, the dynamic equations of the underwater manipulator that consist of pitch-pitch-pitch joints are used to simulate the specified motions.

2.3 Dynamics of UVMS

The dynamic equations for the whole system can be obtained by considering the coupled dynamics between the previously derived dynamic equations of two systems because the movement of one system affects the motion of the other system.[4,10] When an AUV moves with a certain velocity and acceleration, the connecting point between a manipulator and an AUV also has a linear/angular velocity and acceleration. To evaluate the iterative Newton-Euler algorithm, the initial velocity of base-link has to be set as the velocity of the connecting point in order to represent the coupled system. Moreover, since the weight and movement of a manipulator would also affect the AUV dynamics, such forces and moments, calculated through the iterative algorithm should be considered as external forces or disturbances exerted on an AUV in Eq. (12).

$$\sigma = [\sigma_f \quad \sigma_m]^T$$
$$\sigma_f = R_0^B f_1, \quad \sigma_m = R_0^B t_1 - d_{auv/mnp} \times (R_0^B f_1) \tag{12}$$

where σ is the external force vector acting on the vehicle due to the weight and movement of manipulator. The dynamic equations of an AUV including a coupled dynamics with a manipulator can be derived as follows.

$$M_v \dot{\nu} + C_v(\nu)\nu + D_v(\nu)\nu + G_v(\eta) = \tau_v + \sigma \tag{13}$$

Finally, the dynamic equations of the whole system with respect to the body-fixed frame can be written in the form as Eq. (14).

$$M(q)\dot{\zeta} + C(q,\zeta)\zeta + D(q,\zeta)\zeta + G(q,\eta) = \tau$$
$$\zeta = [\nu, \dot{q}]^T, \quad \tau = [\tau_v, \tau_m]^T \tag{14}$$

2.4 Thruster allocation

The AUV to control its 6-DOF motion has seven thrusters. Four horizontal thrusters, which are installed at the bow and the stern part, are operated to control the surge, sway, and yaw motions. Three vertical thrusters enable the AUV to have 3-DOF behaviors of the heave, roll, and pitch motions. Fig. 2 shows the configuration of thrusters. Since the vehicle is equipped with seven thrusters and controlled in 6DOF, the thruster allocation should be conducted as follows.

$$\tau_v = \mathbf{TF};$$
$$\tau_v = [F_x \quad F_y \quad F_z \quad M_x \quad M_y \quad M_z]^T$$
$$\mathbf{F} = [F_1 \quad F_2 \quad F_3 \quad F_4 \quad F_5 \quad F_6 \quad F_7]^T$$
$$\mathbf{T} = \begin{bmatrix} c\alpha & c\alpha & -c\alpha & -c\alpha & 0 & 0 & 0 \\ s\alpha & -s\alpha & s\alpha & -s\alpha & 0 & 0 & 0 \\ 0 & 0 & 0 & 0 & 1 & 1 & 1 \\ 0 & 0 & 0 & 0 & -l_s & l_s & 0 \\ 0 & 0 & 0 & 0 & -l_f & l_f & l_r \\ d_s c\alpha & -d_s c\alpha & -d_s c\alpha & d_s c\alpha & & & \\ +d_f s\alpha & -d_f s\alpha & -d_r s\alpha & +d_r s\alpha & 0 & 0 & 0 \end{bmatrix} \tag{15}$$

where τ_v is the control forces and moments vector acting on the vehicle due to seven thrusters and F is the thrust vector; T is the thruster configuration matrix and α is the angle between the longitudinal axis and direction of the propeller thrust; l_f and l_r are the distance from the center of buoyancy to the vertical thruster at the bow and stern respectively and l_s is the distance from the center line to the vertical thrusters; d_s is the distance from the center of buoyancy to the port and starboard thruster; d_f and d_r are the distance from the center of buoyancy to the horizontal thruster at the bow and stern respectively. In this study, the simplified AUV model in vertical plane used four thrusters to control its 3-DOF motions such as the surge, heave, and pitch motions.

3. Redundancy Resolution

In case of the base-fixed manipulator, the joint trajectories of a manipulator are determined through an inverse kinematics analysis when the trajectory for an end-effector is given. It is also to note that the base of an UVMS is not fixed and floats freely. The trajectory of a vehicle as well as the tip of a manipulator should be predetermined before an inverse kinematics analysis is applied. If the trajectory of a vehicle is not given, the system has a redundancy and the solution of the inverse kinematics is infinite in number. Therefore, the redundancy resolution is introduced to determine the desired trajectories of a manipulator when any specified task is performed.

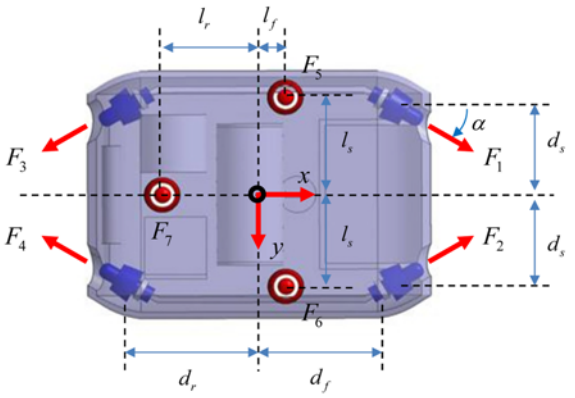

Fig. 2 Thruster configuration

The redundant vehicle-manipulator system may have various combinations of joint velocities that do not affect the given velocity profile of an end-effector and this could induce the self-motion of a vehicle. Hence, by using the degrees of redundancy, the desired trajectories of vehicle and joints can be determined without affecting its motion in the task space.

The relation between the posture of an end-effector and the system configuration can be represented as shown in Eq. (16).

$$\eta_t = f(\eta, q) \tag{16}$$

where $\eta_t \in \Re^{6\times 1}$ is the vector including the position and orientation of an end-effector expressed with respect to the Earth-fixed frame; η and q are the position vector of an AUV and the joint angles vector respectively.

The following equation can be obtained by differentiating Eq. (16) with respect to time.

$$\dot{\eta}_t = \mathbf{J}\begin{bmatrix} \nu \\ \dot{q} \end{bmatrix} = \mathbf{J}\zeta \tag{17}$$

where J is the Jacobian matrix and is a $6\times(6+n)$ matrix in this work. n is the number of joints. When the velocity profile of an end-effector is given, the joint velocities of a manipulator and the velocity of an AUV can be determined by the redundancy resolution.

$$\zeta = \mathbf{J}^{\#}\dot{\eta}_t + (\mathbf{I}_{6+n} - \mathbf{J}^{\#}\mathbf{J})\gamma \tag{18}$$

where $\mathbf{J}^{\#}$ is the Moore-Penrose pseudo-inverse matrix of the Jacobian matrix J and this can be calculated as according to Eq. (19).

$$\mathbf{J}^{\#} = \mathbf{J}^T(\mathbf{J}\mathbf{J}^T)^{-1} \tag{19}$$

The first term in Eq. (18) is the particular solution, which is determined from the given velocity of an end-effector. The second term in Eq. (18) is the homogeneous solution, which is obtained by the projection onto the null-space of Jacobian matrix J. It represents the self-motion which does not affect the task motion. Hence, the vector g

can be defined in order to obtain the optimal solution for the specified performance index.

It is well known that gravity and buoyancy always exert force on all underwater vehicles. Due to these restoring forces and moments, additional control inputs are necessary to maintain the position and orientation of the target. Therefore, the energy consumption associated with a task can be minimized if the restoring forces and moments are minimized and the performance index for minimizing the restoring moments was suggested as represented in Eq. (20).[6]

$$J_{P1} = \frac{1}{2}\left\| \vec{r}_{CG} - \vec{r}_{CB} \right\|^2 \tag{20}$$

where r_{CG} and r_{CB} are the position vector to the center of mass and the center of buoyancy for the whole system with respect to the Earth-fixed frame.

However, the manipulator arms have to be folded as closely as possible toward the hull of the vehicle to minimize the distance between the mass center and buoyancy center if the performance index proposed in the previous work is chosen. This situation might cause the joint limitation of the manipulator arms. Hence, the joint angle constraints should be considered to utilize the performance index with minimizing the restoring moments.

In this study, the additional term for the performance index is presented to avoid the joint limits as follows.

$$J_{p2} = \frac{1}{2}\sum_{i=1}^{n} W_{2i}\left(\frac{2q_i - (q_{i,max} + q_{i,min})}{q_{i,max} - q_{i,min}}\right)^2 = \frac{1}{2} q_J^T W_2 q_J \quad ; \; q_{i,min} \le q_i \le q_{i,max} \tag{21}$$

where q_i denotes the i-th joint variable; $q_{i,min}$ and $q_{i,max}$ represent the lower and upper limits on the joint variable q_i, respectively; W_{2i} is the weight value for the performance index of the i-th joint.

Moreover, it is better to maintain the underwater vehicle with a neutral attitude with respect to the roll and pitch directions in terms of the stability. However, arbitrary values for the roll and pitch directions can be generated through the redundancy resolution using Eq. 20 and Eq. (21) because there are no rules for the generation of the vehicle's attitude. Hence, the constraints for a neutral attitude are added to the performance index to enhance the stability of the underwater vehicle.

$$J_{p3} = \frac{1}{2}\begin{bmatrix}\phi & \theta\end{bmatrix}\begin{bmatrix} W_{31} & 0 \\ 0 & W_{32}\end{bmatrix}\begin{bmatrix}\phi \\ \theta\end{bmatrix} = \frac{1}{2}\eta_J^T W_3 \eta_J \tag{22}$$

where ϕ and θ denote the roll and pitch angle of the vehicle with respect to the Earth-fixed frame, respectively; W_3 is the weight matrix.

Finally, the performance index for the redundancy resolution is proposed as follows in this study.

$$J_p = \frac{1}{2}\Gamma^T W_p \Gamma$$

$$; \quad \Gamma = \begin{bmatrix}\left\| \vec{r}_{CG} - \vec{r}_{CB} \right\| & q_J & \eta_J\end{bmatrix}^T \qquad W_p = \begin{bmatrix} W_1 & 0 & 0 \\ 0 & W_2 & 0 \\ 0 & 0 & W_3 \end{bmatrix} \tag{23}$$

where W_P is the weight matrix, which is both symmetric and positive.

Hence, the vector γ for obtaining the optimal solution can be determined using the gradient projection method and the predefined performance index function.

$$\gamma = -\kappa \cdot \nabla J_P \tag{24}$$

where κ is the gradient gain with a positive sign; ∇J_P is the gradient of the performance index function J_P.

4. Controller Design

In order to track the desired trajectories of a vehicle and joints, determined through the redundancy resolution, attempts have been made to suitably design the sliding mode controller in the current work. The dynamic equations for the whole system expressed in Eq. (14) have some properties as follows.

- property 1: The inertia matrix $M(q)$ of the whole system is symmetric and positive definite: $M = M^T > 0$

This means the all eigenvalues of the matrix M are greater than zero: $0 < \lambda_{min}(M) \le \|M\| \le \lambda_{max}(M)$

- property 2: $\dot{M} - 2\dot{C}$ is skew-symmetric: $x^T[\dot{M} - 2C]x = 0$
- property 3: The matrix $D(q, \zeta)$ is positive definite: $D > 0$
- property 4: Assume that the model uncertainties are bounded by some known functions. ^ denote the estimated system matrices and ~ represent the estimation error matrices.

$$\|\tilde{M}\| = \|M - \hat{M}\| \le \Delta_M < \infty \quad \|\tilde{C}\| = \|C - \hat{C}\| \le \Delta_C < \infty$$
$$\|\tilde{D}\| = \|D - \hat{D}\| \le \Delta_D < \infty \quad \|\tilde{G}\| = \|G - \hat{G}\| \le \Delta_G < \infty$$

The sliding mode control law can be chosen as shown in Eq. (25) in order to follow the desired trajectories of the vehicle and manipulator joints.

$$\tau = \hat{M}(\ddot{\zeta}_d + \Lambda\dot{e}) + (\hat{C} + \hat{D})(\dot{\zeta}_d + \Lambda e) + \hat{G} + K_1 s + K_2 sgn(s) \tag{25}$$

where K_1 and K_2 are positive definite matrices of gains; $sgn(s)$ is a sign function; the subscript d means the desired value, and Λ is a positive definite gain matrix. An error vector $e(t)$ of the vehicle posture and the joint angles and the sliding manifold $s(t)$ are defined in Eq. (26).

$$e(t) = \begin{bmatrix} R_E^B(\eta_d - \eta) \\ q_d - q \end{bmatrix}$$
$$s(t) = \dot{e}(t) + \Lambda e(t) = \zeta_d(t) - \zeta(t) + \Lambda e(t) \tag{26}$$

where R_E^B is the rotation matrix from the Earth-fixed frame to the body-fixed frame.

To assure the stability of the proposed sliding mode control law, a quadratic Lyapunov function candidate can be defined as Eq. (27). The proposed function is positive definite by the property 1.

$$V = \frac{1}{2} s^T M s > 0 \tag{27}$$

Differentiating V with respect to time, Eq. (28) can be obtained as follows.

$$\dot{V} = \frac{1}{2} s^T \dot{M} s + s^T M \dot{s} \tag{28}$$

From the time-varying differential equation of the sliding manifold $s(t)$ and the dynamic equations of UVMS expressed in Eq. (14), Eq. (28) can be rewritten as Eq. (29).

$$\dot{V} = \frac{1}{2}s^T\dot{M}s + s^T M[M^{-1}\{(C+D)\zeta + G - \tau\} + \dot{\zeta}_d + \Lambda\dot{e}] \quad (29)$$

Eq. (30) is also obtained by taking into account the property 2 and Eq. (26).

$$\dot{V} = -s^T Ds + s^T[M(\dot{\zeta}_d + \Lambda\dot{e}) + (C+D)(\zeta_d + \Lambda e) + G - \tau] \quad (30)$$

The designed control law represented in Eq. (25) is substituted into the Eq. (30), which yields the closed-loop equation, as follows.

$$\begin{aligned}\dot{V} = &-s^T(D+K_1)s - s^T K_2 \mathrm{sgn}(s) \\ &+ s^T[\tilde{M}(\dot{\zeta}_d + \Lambda\dot{e}) + (\tilde{C}+\tilde{D})(\zeta_d + \Lambda e) + \tilde{G}]\end{aligned} \quad (31)$$

In view of properties 1, 3 and the positive definiteness of gain matrices K_1 and K_2, the function $\dot{V}$ can be upper bounded as shown in Eq. (32).

$$\begin{aligned}\dot{V} \le &-\lambda_{\min}(D+K_1)\|s\|^2 - \lambda_{min}(K_2)\|s\| \\ &+ \left\|s^T[\tilde{M}(\dot{\zeta}_d + \Lambda\dot{e}) + (\tilde{C}+\tilde{D})(\zeta_d + \Lambda e) + \tilde{G}]\right\|\end{aligned} \quad (32)$$

By property 4 and a triangle inequality condition, the inequality can be rewritten as follows.

$$\begin{aligned}\dot{V} &\le -\lambda_{min}(D+K_1)\|s\|^2 - \lambda_{min}(K_2)\|s\| \\ &\quad + (\|\tilde{M}\|\|\dot{\zeta}_d + \Lambda\dot{e}\| + (\|\tilde{C}\| + \|\tilde{D}\|)\|\zeta_d + \Lambda e\| + \|\tilde{G}\|)\|s\| \\ &\le -\lambda_{min}(D+K_1)\|s\|^2 - \lambda_{min}(K_2)\|s\| \\ &\quad + (\Delta_M\|\dot{\zeta}_d + \Lambda\dot{e}\| + (\Delta_C + \Delta_D)\|\zeta_d + \Lambda e\| + \Delta_G)\|s\|\end{aligned} \quad (33)$$

where λ_{min} means the smallest eigenvalue of the corresponding matrix.

By choosing K_2 such that

$$\lambda_{min}(K_2) \ge \Delta_M\|\dot{\zeta}_d + \Lambda\dot{e}\| + (\Delta_C + \Delta_D)\|\zeta_d + \Lambda e\| + \Delta_G \quad (34)$$

the time derivative of the positive definite function V is negative definite and thus the sliding manifold $s(t)$ tends to zero asymptotically. Thus, the designed sliding mode controller satisfies the stability against any uncertainty for the manipulator arm such as the object with an unknown mass. The sign function in Eq. (25) can be replaced by a saturation function to prevent a chattering phenomenon.

The optimal inputs for seven thrusters were calculated through the thruster configuration matrix as described in Eq. (15). In this study, the inputs for four thrusters were determined to control the 3-DOF motions in vertical plane.

$$\mathbf{F} = \mathbf{T}^{\#} \cdot \tau_v = \mathbf{T}^T(\mathbf{T}\mathbf{T}^T)^{-1} \cdot \tau_v \quad (35)$$

where $T^{\#}$ is the pseudo-inverse of the thruster configuration matrix T.

5. Simulations

To verify the effectiveness of the proposed redundancy resolution and the control algorithms, the 3DOF vehicle-3DOF manipulator planar model shown in Fig. 3 was formed and the proposed algorithms were applied to this model. The parameters for the underwater vehicle and manipulator used in the simulations are shown in Table 1.

In the first simulation, the underwater vehicle locates at the initial position (0,0) in the vertical plane with a zero pitch angle and the joints

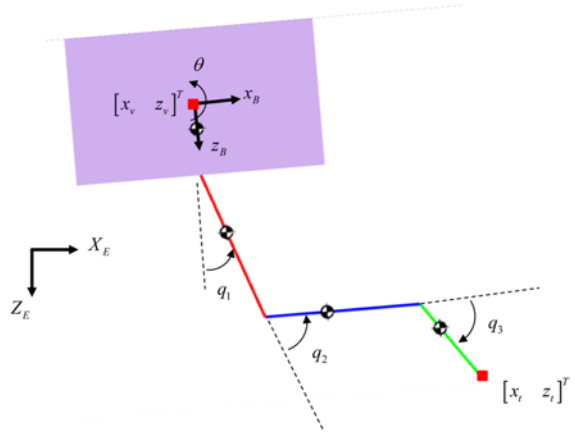

Fig. 3 3DOF vehicle-3DOF manipulator planar model

Table 1 Parameters for the underwater vehicle and manipulator

		Values
Vehicle	L × H × W	0.8 × 0.5 × 0.6 [m]
	Mass	80.5 [kg]
	Moment of inertia	26.1 [kg·m^2]
Link1	Mass	10 [kg]
	Length	0.5 [m]
Link2	Mass	10 [kg]
	Length	0.5 [m]
Link3	Mass	5 [kg]
	Length	0.3 [m]

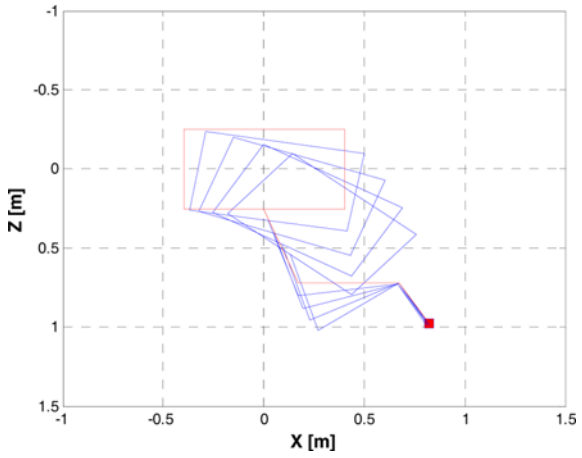

Fig. 4 Stick diagram of the vehicle and manipulator

of the manipulator have the initial angles such as 20°, 70°, -60°, respectively.

From the initial joint variables, the position of the end-effector can be calculated using the forward kinematics. The joints as well as the underwater vehicle have to move for minimizing the restoring moments acting on the whole system if the end-effector should be kept at the initial position and orientation. However, the performance index presented in Eq. (20) does not have any constraints for the orientation of the vehicle and the joint limits. Hence, the vehicle could have the pitch angle during optimizing the performance index to minimize the

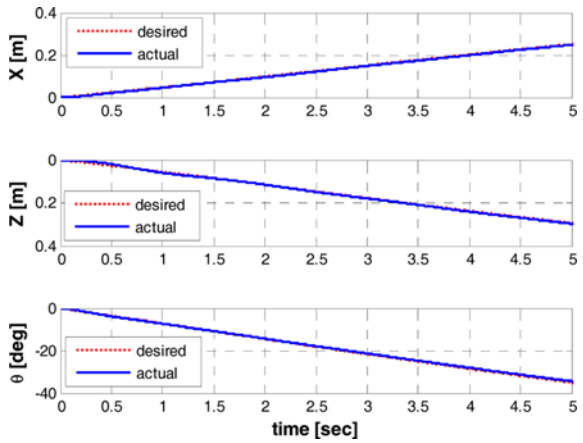

Fig. 5 Position and orientation of the vehicle

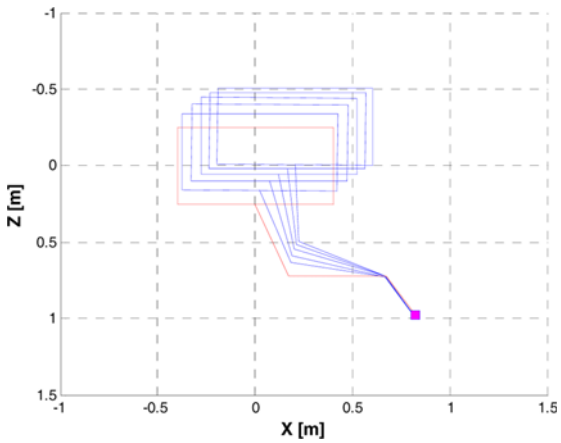

Fig. 7 Stick diagram of the vehicle and manipulator (proposed)

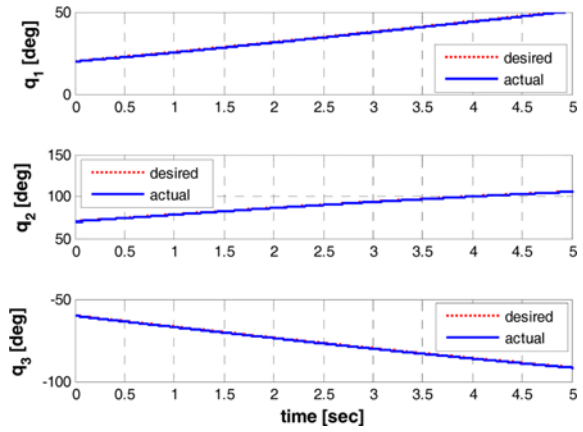

Fig. 6 Joint variables of the manipulator

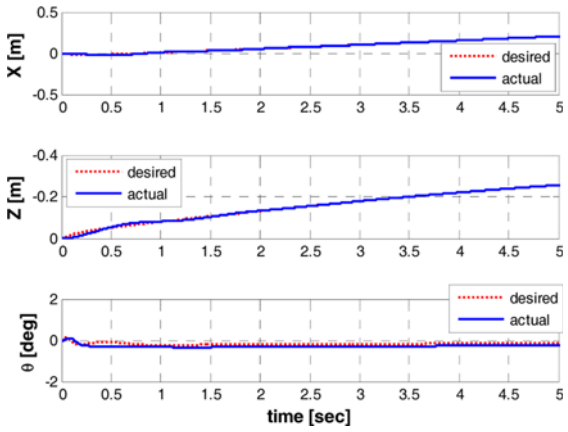

Fig. 8 Position and orientation of the vehicle (proposed)

restoring moments and the joint limits could be exceeded.

Fig. 4 shows the stick diagram of the whole system during the first simulation. It is clear that the underwater vehicle rotates during the optimization as shown in the plot. The position and orientation of the underwater vehicle generated through the redundancy resolution are represented by red dotted lines and the controlled trajectories by the sliding mode controller are shown by blue solid lines in Fig. 5. The pitch angle of the vehicle reaches to about -35° after 5 seconds and this means a large amount of pitch angle might cause the instability of the whole system. Fig. 6 also shows the joint variables of the manipulator obtained by the trajectory generator (redundancy resolution) and the controlled joint variables by the proposed controller. The second and third joint angles exceed the 100° and -90° after 5 seconds, respectively. If the joint angles of the manipulator have to remain between -90° and 90°, these results will induce the unpredictable and unwanted motion of the whole system.

To prevent these situations, the proposed algorithm in this study is used to generate the trajectories of the vehicle and the joint angles of the manipulator. To enhance the stability of the system, the underwater vehicle should maintain the neutral attitude with a zero pitch angle. Moreover, the manipulator has to have the motion inside the bounded region. The simulation under an identical condition as in the previous

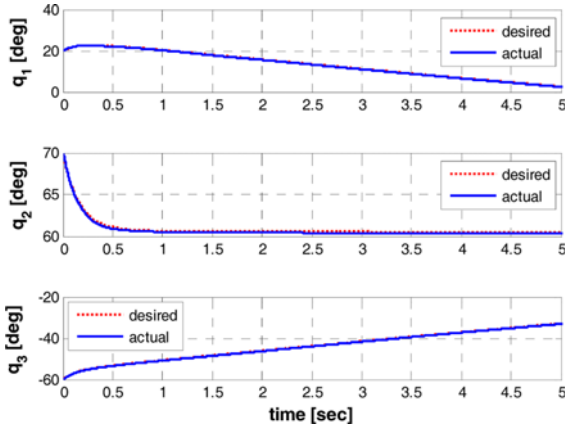

Fig. 9 Joint variables of the manipulator (proposed)

case is conducted to verify the effectiveness of the proposed algorithm. Fig. 7 shows the simulation result for the stick diagram obtained using the proposed algorithm.

It is obvious that the vehicle maintains the neutral attitude in terms of the pitch angle as shown in Fig. 7. Figs. 8 and 9 represent the trajectories of the vehicle and joints generated by the redundancy

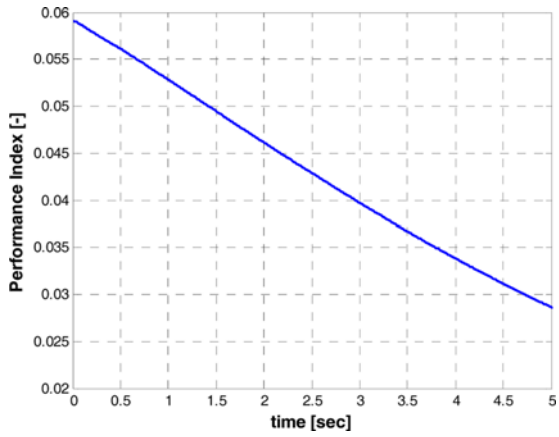

Fig. 10 Performance index value (proposed)

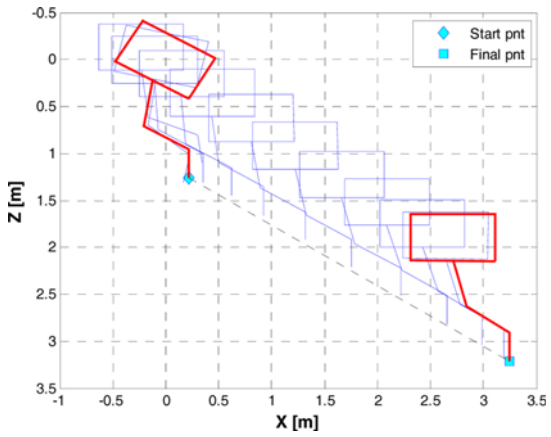

Fig. 11 Stick diagram of UVMS (unknown parameter)

resolution for the proposed performance index, respectively. The pitch angle of the vehicle is maintained around a zero and all joint angles generated by the trajectory generator satisfy the joint constraints, which are determined $-80^{o} \le q_i \le 80^{o}$; $i = 1, 2, 3$. Fig. 10 shows the variation of the performance index with time, while the trajectory tracking control is being applied to the whole system. The plot shows that the proposed performance index decreased monotonically with time in case of using the optimization, which implied the minimization of the restoring moments while the joint constraints and the minimization of the pitch angle are being satisfied.

Next, the robustness for the tracking controller with parameter uncertainties is verified through a simulation. The trajectory of the end-effector is assigned to move along a straight line from the initial position to the end position with a cubic polynomial velocity profile for 6 seconds. The manipulator starts its motion from its initial position (x_t =0.22 m, z_t=1.26 m) and orientation of the tip (q_t=-20°) with unknown mass object of 10 kg. The end-effector of the manipulator moves to the target position (x_t=3.22 m, z_t=3.26 m) and target orientation of q_t=0°. Fig. 11 shows the simulation result for the trajectory tracking control with parameter uncertainty. The tip position tracks well along a straight line from the initial position to the final position with a zero tip orientation. Besides, the pitch angle of the vehicle almost maintains the neutral attitude to improve the dynamic stability with satisfying the joint constraints.

Figs. 12 and 13 represent the desired and controlled trajectories of the vehicle and all joints of the manipulator through the proposed algorithms. In the beginning, the large pitch angle of the vehicle and errors of joint variables generate due to the object with an unknown mass. However, the neutral attitude and proper joint angles are generated by the suggested redundancy resolution and these tracking errors decrease rapidly by the sliding mode control law.

The simulation results confirm that the actual trajectories could track the desired trajectories efficiently from the start point to the end point by the designed controller and redundancy resolution despite a parameter uncertainty. Fig. 14 shows the variation of the performance index with time, while the trajectory tracking control is being applied to the system.

The plot shows that the proposed performance index decreased monotonically with time in case of using the optimization. On the other

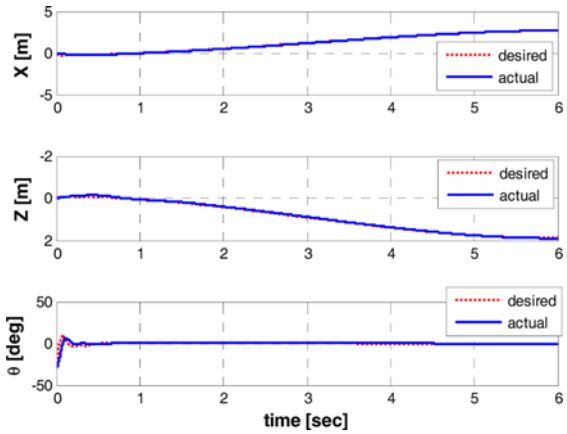

Fig. 12 Underwater vehicle variables (unknown parameter)

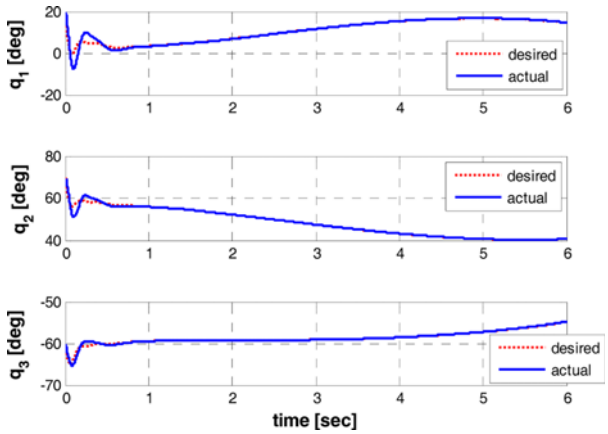

Fig. 13 Joint variables of the manipulator (unknown parameter)

hand, the performance index for using the only inverse kinematics does not decrease. The results using the proposed performance index, in turn, would save the inputs required to control the position and orientation of the whole system. The forces for the four thrusters along with the joint torques are finally shown in Figs. 15 and 16. As the results are shown, the control inputs for the proposed algorithm are smaller than

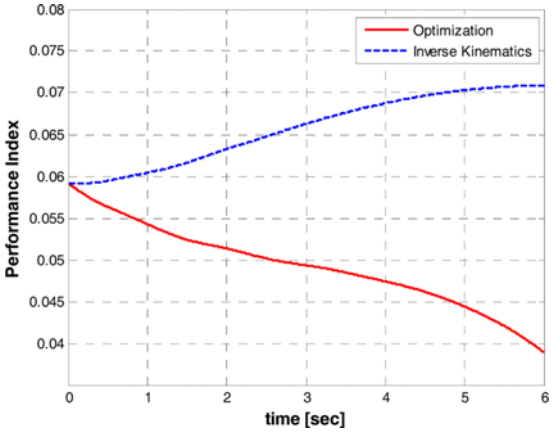

Fig. 14 Variation of the Performance index with time

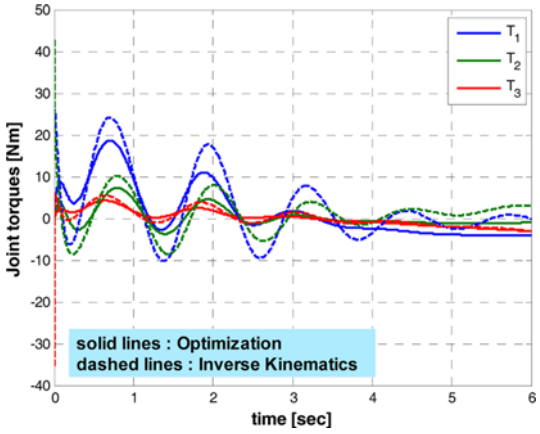

Fig. 16 Joint torques of the manipulator

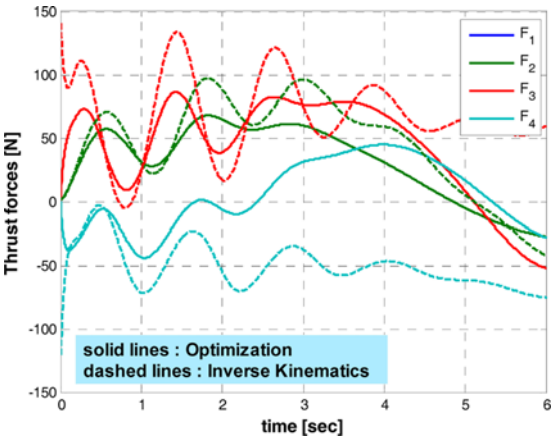

Fig. 15 Thruster forces of the vehicle

those for the only inverse kinematics analysis. Therefore, the proposed method can be more advantageous in terms of power saving.

6. Conclusions

The study on trajectory generation and control algorithm of an UVMS with redundancy has been conducted in this paper. The performance index was defined to minimize the restoring moments acting on the system while maintaining the neutral attitude of the underwater vehicle to improve the dynamic stability and satisfying the joint constraints. By applying the proposed control algorithms, the inputs required to control the whole system decreased. To satisfy this purpose, the desired optimal trajectories of the system were generated through the redundancy resolution and robust control algorithms were proposed to track the generated trajectories. Simulation results show the validity of the proposed algorithms.

ACKNOWLEDGEMENT

This research was a part of the project titled ‘R&D center for underwater construction robotics’, funded by the Ministry of Oceans and Fisheries (MOF) and Korea Institute of Marine Science & Technology Promotion (KIMST), Korea (PJT200539). Also, it was supported by National Emergency Management Agency (2012-NEMA10-004-01010 002-2012).

REFERENCES

1. Antonelli, G. and Chiaverini, S., “Task-Priority Redundancy Resolution for Underwater Vehicle-Manipulator Systems,” Proc. of the IEEE International Conference on Robotics and Automation, pp. 768-773, 1998.
2. Antonelli, G., “Underwater Robots Motion and Force Control of Vehicle-Manipulator Systems,” Springer, pp. 109-111, 2006.
3. Craig, J. J., “Introduction to Robotics: Mechanics and Control,” Addison-Wesley, pp. 196-200, 1989.
4. Dunnigan, M. W. and Russell, G. T., “Evaluation and Reduction of the Dynamic Coupling between a Manipulator and an Underwater Vehicle,” IEEE Journal of Oceanic Engineering, Vol. 23, No. 3, pp. 260-273, 1998.
5. Fossen, T. I., “Guidance and Control of Ocean Vehicles,” John Wiley & Sons, pp. 5-56, 1994.
6. Han, J., Park, J., and Chung, W. K., “Robust Coordinated Motion Control of an Underwater Vehicle-Manipulator System with Minimizing Restoring Moments,” Ocean Engineering, Vol. 38, No. 10, pp. 1197-1206, 2011.
7. Hollerbach, J. and Suh, K., “Redundancy Resolution of Manipulators through Torque Optimization,” IEEE Journal of Robotics and Automation, Vol. 3, No. 4, pp. 308-316, 1987.
8. Kim, J., Marani, G., Chung, W. K. and Yuh, J., “Task Reconstruction Method for Real-Time Singularity Avoidance for Robotic Manipulators,” Advanced Robotics, Vol. 20, No. 4, pp. 453-481, 2006.
9. Marani, G., Choi, S. K., and Yuh, J., “Underwater Autonomous

Manipulation for Intervention Missions AUVs," Ocean Engineering, Vol. 36, No. 1, pp. 15-23, 2009.

10. Mohan, S. and Kim, J. H., "Indirect Adaptive Control of an Autonomous Underwater Vehicle-Manipulator System for Underwater Manipulation Tasks," Ocean Engineering, Vol. 54, pp. 233-243, 2012.

11. Sakar, N. and Podder, T., "Coordinated Motion Planning and Control of Autonomous Underwater Vehicle-Manipulator Systems Subject to Drag Optimization," IEEE Journal of Oceanic Engineering, Vol. 26, No. 2, pp. 228-239, 2001.

12. Schjølberg, I. and Fossen, T. I., "Modelling and Control of Underwater Vehicle-Manipulator Systems," Proc. of the 3rd Conference on Marine Craft Maneuvering and Control, pp. 45-57, 1994.